Journal of The Electrochemical Society, **152** (4) A767-A773 (2005)
0013-4651/2005/152(4)/A767/7/$7.00 © The Electrochemical Society, Inc.

Ceramic-Polymer Electrolytes for All-Solid-State Lithium Rechargeable Batteries

Guoxin Jiang,[a] Seiji Maeda,[b] Yoichiro Saito,[b] Shigeo Tanase,[a,*] and Tetsuo Sakai[a,*,z]

[a]*National Institute of Advanced Industrial Science and Technology, Research Institute for Ubiquitous Energy Devices, Research Team of Secondary Battery System, Ikeda, Osaka 563-8577, Japan*
[b]*The Nippon Synthetic Chemical Industry Company, Limited, Ibaraki, Osaka 567-0052, Japan*

New polyurethane acrylate (PUA)-based nanoceramic-polymer electrolytes in a high ceramic filler content were examined in all-solid-state lithium-polymer cells (Li/PUA-SiO_2/$Li_{0.33}MnO_2$) and at 60°C. The composite electrolyte containing more than 20 wt % hydrophilic nano-SiO_2 enhanced its mechanical strength 600% compared to the ceramic-free electrolyte. The additions of nano-SiO_2 powders in a high concentration protected the electrode surfaces, improved greatly the interfacial stability between composite cathode and the electrolyte, and gave rise to a further reversible lithium stripping-deposition process. The cells showed good rate capacity and excellent cyclability. The discharge capacity kept 65% of initial capacity after 300 cycles with a coulombic efficiency approaching 100%. Capacity fading upon cycling was believed to be due to the increase of cell resistance during charge-discharge cycling. The cell self-charge loss at 60°C was extremely low about 0.05% per day.
 [DOI: 10.1149/1.1865892]

Manuscript submitted April 28, 2004; revised manuscript received October 13, 2004. Available electronically March 7, 2005.

A challenging goal in lithium battery technology, especially for electric vehicle applications, is the use of a metallic lithium anode and a solid polymer electrolyte instead of a carbon anode and a liquid electrolyte, *i.e.*, developing a true solid lithium polymer battery (LPB) from a liquid-electrolyte lithium ion battery (LIB), because of its advantages of improved safety, high energy density, and flexibility. The concept was first proposed by Armand and coworkers in 1979.[1] One key component of the lithium polymer battery is the polymer electrolyte. The proper choice of the component is ruled by a series of requirements which include high ionic conductivity, good mechanical properties, and compatibility with the electrode materials. In recent years, large research efforts have been devoted to improving the properties of the polymer electrolytes to satisfy the need of all solid-state lithium polymer battery.[2-5] The main problem associated with such type of battery is the low ionic conductivity of the polymer electrolyte and the poor characteristics of the interface between lithium and polymer electrolyte. One of the most successful ways is the introduction of ceramic fillers (such as SiO_2, TiO_2, Al_2O_3, γ-$LiAlO_2$),[6-10] which results in an enhanced ionic conductivity and an improved interfacial stability between lithium and polymer electrolyte.

As the surface groups of SiO_2 powders can be modified to tailor the interfacial properties for a specific need, many works have been carried out about effects of SiO_2 powders on the properties of polymer electrolytes.[11-16] Although not all of the previous experimental results are unanimous about the functions and effects of SiO_2 powders, the addition of SiO_2 can greatly improve the interface stability between lithium and polymer electrolyte. However, in the previous researches, there are hardly studies about the amount of SiO_2 powder filler in excess of 10 wt % until a recent report by the NCSU group.[24] In addition, there are few reports about the study of interface stability between the polymer electrolyte and composite cathode, which is one of the most important problems in a practical battery system.

In a previous study,[17] we have discussed the effects of hydrophobic and hydrophilic nano-SiO_2 powders (filler content was no more than 10 wt %) on the properties of polymer electrolyte. We found that hydrophilic nano-SiO_2 powders enhanced strongly the mechanical property of polymer electrolyte, and improved greatly the interfacial stability between lithium anode and polymer electrolyte. However, the interface between composite cathode ($Li_{0.33}MnO_2$) and polymer electrolyte was still unstable even after the addition of nano-SiO_2 powders, and strongly influenced the cyclic performance of cells.

In this paper, we report the most recent results obtained in our laboratory on the characterization of all-solid-state lithium polymer battery with nano-SiO_2 composite polymer electrolytes. We for the first time introduce 20-40 wt % nano-SiO_2 powders to polymer electrolyte (PUA) as a ceramic nano-composite polymer electrolyte for all-solid-state lithium polymer battery. The cyclic performance of these cells with the nano-composite polymer electrolyte is also investigated in details. We found that the interfaces (between composite cathode and polymer electrolyte, or between lithium and polymer electrolyte) were extremely stable after adding more than 20 wt % hydrophilic nano-SiO_2 powders. The discharge capacity of these cells could keep at 160 mAh/g (no decrease) after more than 100 cycles. We believe that a practical all-solid-state lithium polymer battery with a nano-ceramic polymer electrolyte will come into being in the near future.

Experimental

Polymer electrolyte films used here were prepared by a solvent-free casting technique in dry air.[18,19] Urethane acrylate (UA) oligomer was synthesized from 2-Hydroxyethyl acrylate, Isophorone diisocyanate (IPDI) and P(EO/PO). The detailed synthesis and polymerization procedure of the poly(urethane acrylate) (PUA) is illustrated in Schemes 1 and 2.

Urethane acrylate (UA) was synthesized by two consecutive steps. First, a prepolymer was formed by the reaction of isophorone diisocyanate(IPDI) (Degussa Japan; 97 g) with polyoxyethylene polyoxypropylene glycol(P(EO/PO) (Asahi Denka; 870 g) at 90°C for 4 h under a dry nitrogen atmosphere. Then, 2-hydroxyethyl acrylate (2HEA) (Osaka Organic Chemical industry; 33 g) was added to the prepolymer, and to react at 60°C for 14 h. At the end of reactions, chemical analysis and infrared (IR) spectrophotometry were used to measure the remains of NCO. That low molecular weight materials did not generate was also confirmed with the measurement of size exclusion chromatography (SEC).

Then, methoxypolyethylene glycol monoacrylate (Mw = 636) (NOF Corporation, 30 g) as a polymerizable viscosity reducer, LiTFSI [$LiN(CF_3SO_2)_2$] (Kishida Chemical) as a Li salt, and 1-hydroxy cyclohexyl phenyl ketone as a photoinitiator(Ciba Specialty Chemicals, 0.5 g) were dissolved into the above urethaneacrylate (70 g), and stirred continuously at room temperature until forming a homogenous mixture. The salt concentration was fixed at O/Li = 20/1 for the polymer electrolyte. The mixture then was irradiated by UV light to yield homogenous and mechanically stable

* Electrochemical Society Active Member.
z E-mail: sakai-tetsuo@aist.go.jp

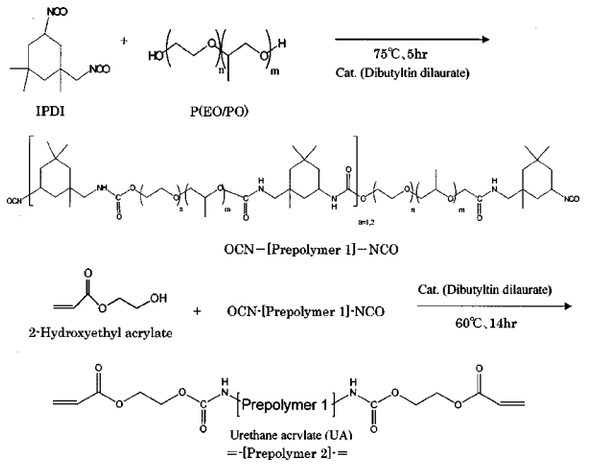

Scheme 1.

membranes of average thickness of 100 μm. Nano-composite polymer electrolytes were prepared by mixing nano-size SiO_2 (AEROSIL300 NIPPON AEROSIL) powders to the above polymer electrolyte before the UV radiation, using a special Conditioning Mixer (THINKY, AR-250) in a dry room with a dew point lower than −60°C. Nano-size SiO_2 powders were dried at 160°C under vacuum for 48 h before use. Table I lists samples and some properties of SiO_2 powders.

The cathode material, $Li_{0.33}MnO_2$, was prepared by preheating a mixture of $LiNO_3$ and MnO_2 at 260°C for 5 h, followed by heating at 320°C for 12 h in air.[20] The composite cathode was prepared by mixing proper amounts of $Li_{0.33}MnO_2$ with PEG [poly(ethylene glycol), Mw = 2000], LiTFSI and carbon (Ketjen black). The mixture was strongly stirred before casting on the aluminum substrate. After the cathode composite material was dried at 80°C under vacuum for 48 h, it was pressed into a thin film of about 50 μm in thickness. The

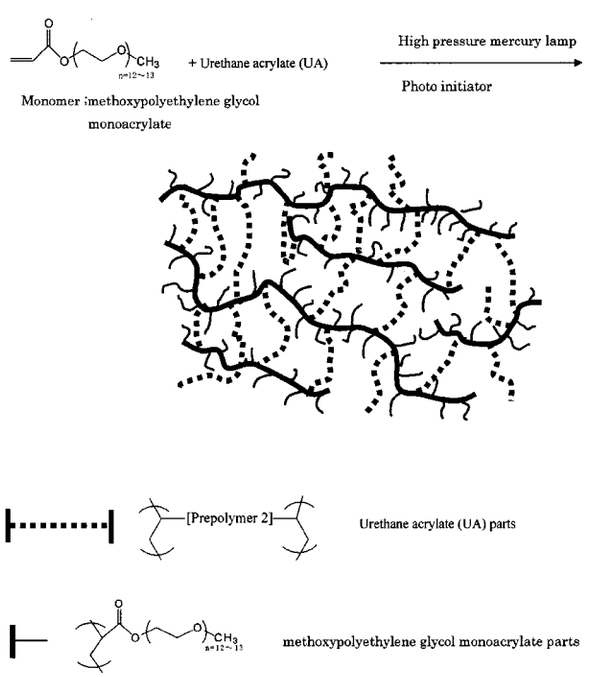

Scheme 2.

Table I. Properties of SiO_2 ceramic additives.

Sample	Amount (wt %)	Size (nm)	Surface area (m^2/g)	Surface groups	Type of surface
PUA	0				
PUA10	9.1	7	300	Si-OH	Hydrophilic
PUA20	16.7	7	300	Si-OH	Hydrophilic
PUA30	23.1	7	300	Si-OH	Hydrophilic
PUA40	28.6	7	300	Si-OH	Hydrophilic
PUA50	33.3	7	300	Si-OH	Hydrophilic

typical weight ratio of active material, carbon, and PEG_{20}-LiTFSI in the cathode mixture was 65, 5 and 30 wt %, respectively.

The electrical conductivity of the polymer electrolyte films and the interfacial resistance between the electrolyte and the electrodes (the Li metal anode and the composite cathode) were measured by an ac impedance method using a Solartron 1260 frequency analyzer. Stainless steel blocking electrode cells were used for conductivity measurements, and symmetrical nonblocking lithium electrode (or the composite cathode) cells were used to investigate the interfacial phenomena. The ac oscillation amplitude was 10 mV, and the impedance spectra were collected by recording 10 points per decade over a frequency range from 10 KHz to 0.1 Hz in conductivity measurements, and from 100 KHz to 0.1 Hz in interfacial resistance measurements.

The lithium ion transference number (t^+) was determined using the dc polarization/ac impedance combination method.[21] A constant potential of 10 mV was applied to the electrodes for the polarization.

The dynamic Young's modulus of nano-ceramic polymer electrolyte membranes was measured using a DVA-225 (ITK Co. Ltd) at a frequency of 10 Hz with a heating rate of 2.5°C/min.

Test cells were assembled by sandwiching the polymer electrolyte film between a lithium foil and the composite electrode. The charge/discharge performance tests of the cells were performed galvanostatically at a current rate of C/4 (0.05 mA/cm^2, 50 mA/g) and at a regulated cut-off voltage between 2.0 and 3.5 V at 60°C.

Results and Discussion

Mechanical property.—Good mechanical strength is required for use as an electrolyte separator in the lithium/polymer battery production process. The dynamic Young's moduli of nano-composite polymer electrolytes with various amounts of SiO_2 powders were

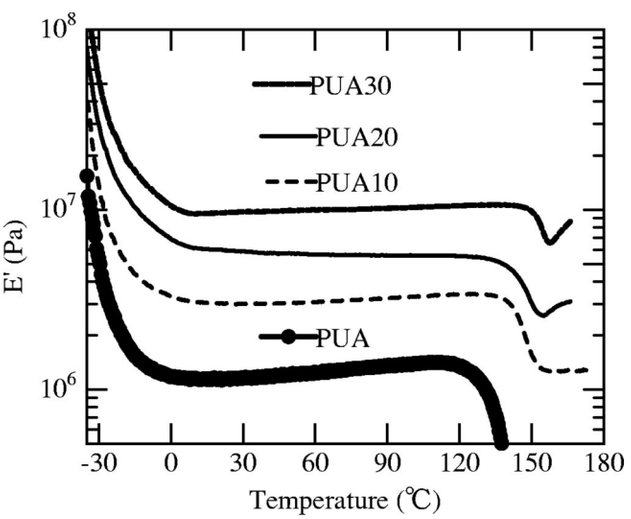

Figure 1. Dynamic moduli of polymer electrolyte films with various amounts of hydrophilic SiO_2 powders.

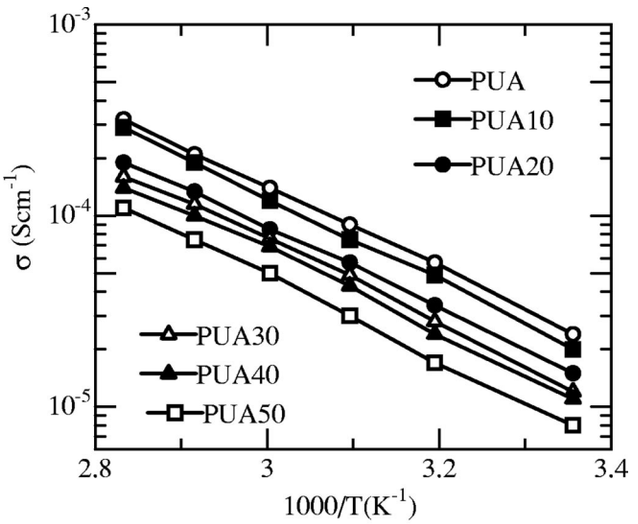

Figure 2. Temperature dependence of ionic conductivity of ceramic-polymer electrolytes with various amounts of SiO_2 powders.

investigated in comparison with the ceramic-free electrolyte (PUA), as shown in Fig. 1. The addition of hydrophilic nano-SiO_2 powders more than 20 wt % enhanced the mechanical strength of electrolyte ten times comparing to the ceramic-free electrolyte. Also, the ceramic-polymer electrolyte possessed good mechanical properties even above 150°C. It is possible for the ceramic-polymer electrolyte to be used as an electrolyte separator in the lithium/polymer battery, if the addition of SiO_2 powders is more than 20 wt %.

Conductivity and lithium transference number.—We investigated the effects of hydrophilic nano-SiO_2 powders at high loadings on the ionic conductivity of polymer electrolyte. Figure 2 shows the temperature dependence of ionic conductivity of the ceramic-polymer electrolytes with various amounts of SiO_2 powders. According to the results, all samples had the similar activation energy. This suggests that the local dynamics of lithium-ion transport was not changed. The addition of nano-SiO_2 powders did not alter the mechanism for ion conduction in the PUA system. However, high loadings of ceramic fillers did not enhance ionic conductivity of the

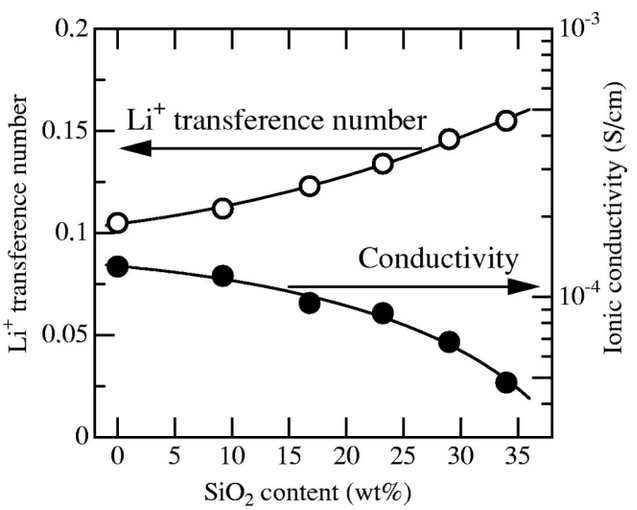

Figure 3. Relationships between the amount of SiO_2 powders and ionic conductivity and Li^+ transport number at 60°C.

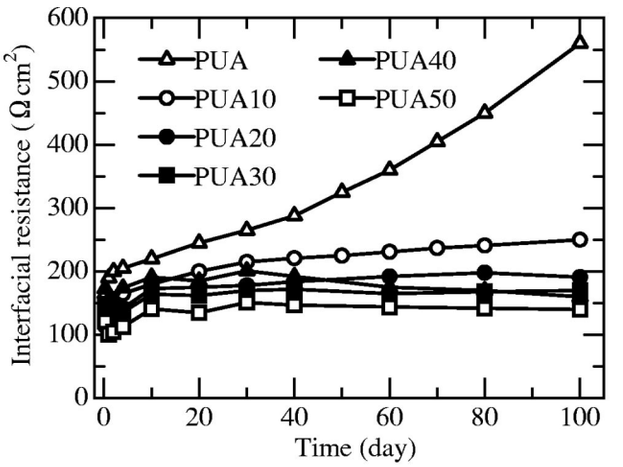

Figure 4. Time dependence of interfacial resistances of the Li/PUA-SiO_2/Li cell stored in OCV conditions at 60°C.

polymer electrolyte, but lower its conductivity slightly. The sensitivity of filler content to conductivity of composite electrolytes shows the similar result with a recent report using fumed oxide fillers (SiO_2, Al_2O_3, and TiO_2).[25] The effect of SiO_2 content on conductivity does not apparently scale with volume fraction of filler. Before explaining the phenomenon, we checked the lithium ion transport number in the ceramic-polymer electrolyte.

Figure 3 shows the relationships between the amount of adding SiO_2 and the conductivity and the lithium ion transport number at 60°C. The ionic conductivity of ceramic polymer electrolytes decreased with the increase of ceramic filler content. At high ceramic filler concentrations, the low conductivities were caused by dilution effects and phase discontinuities. However, the Li ion transport number did not decrease, but increased with the increase of ceramic filler concentration. In the PUA electrolytes, Li^+ ions were coordinated to oxygen atoms in the polymer chains. The movement of dissociated Li^+ ions can be constrained by multiple oxygen atoms coordinated to the same central Li ions. Upon the addition of hydrophilic nano-SiO_2, the oxygen atoms from the SiO_2 units in the vicinity of SiO_2 surface may compete with oxygen atoms from (EO)n in the PUA backbone for coordination with Li^+ ions. This results in a more relaxed coordination between oxygen atoms and Li^+ ions, which facilitates the transport of Li^+ ions through the polymer.[10] Thus, the decrease of ionic conductivity of the composite polymer electrolytes is mainly due to the decrease of anion $[N(CF_3SO_2)_2^-]$ conduction with the increase of ceramic filler content, *i.e.*, high ceramic filler content obstructs the anion transport.

Interfacial stability with metallic lithium and cathode.—The interfacial stability between the ceramic-polymer electrolytes and the lithium anode was investigated on symmetric Li/PUA-SiO_2/Li cells by following the evolution of both the interfacial impedance under open-circuit condition and the cell overvoltage during consecutive plating-stripping cycles.

Figure 4 shows the evolution of the interfacial resistance with time for all samples at 60°C. In our previous report,[17] the addition of nano-SiO_2 powders significantly lowers the increase of the interfacial resistance with time. From the results in Fig. 4, the addition of more than 20 wt % nano-SiO_2 powders could completely control the increase of the interfacial resistance with time. Even after two months of initial passivation of the Li/ceramic-polymer electrolyte interface, the value of the interfacial resistance did not change. Because it is reasonable to assume that the increase of the interfacial resistance is due to the progressive growth of the passivation film, no growth in the interfacial resistance after the addition of more than 20 wt % nano-SiO_2 powders indicates a stabilized Li/electrolyte

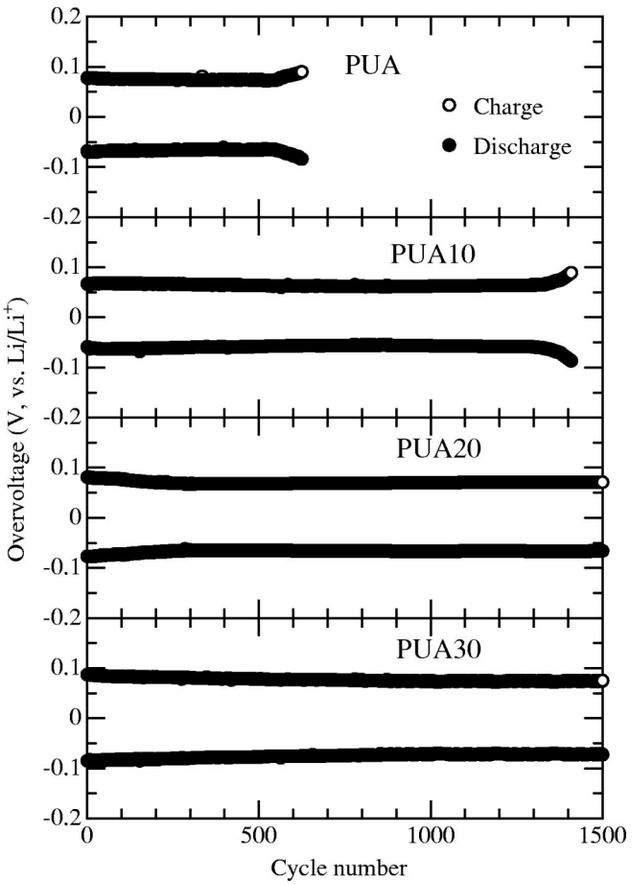

Figure 5. Change in the overvoltage upon cycling of symmetric Li/ PAU-SiO_2/Li cells containing various electrolytes at 60°C. Cell was cycled at a current density of 0.1 mA/cm^2 for 1 h.

interface. This allows us to predict that batteries using such a ceramic-polymer electrolyte would show high storage stability even at the operating temperature.

The interfacial stability between the ceramic-polymer electrolyte and metallic lithium was also evaluated in kinetic conditions, *i.e.*, during the lithium oxidation and reduction at two Li electrodes, by means of galvanostatic plating/stripping tests. Figure 5 gives the overvoltage evolution associated with the galvanostatic cycle test on a symmetric Li/PUA-SiO_2 electrolytes/Li cell. The test was conducted using a constant current (0.1 mA/cm^2) through the cell for 1 h in each direction at 60°C. During the lithium plating and stripping cycles, a passivation layer at the lithium-electrolyte interface is continuously formed and disrupted. The increase of the overvoltage at the end of each plating-stripping cycle is relative to the formation and variation of the passivation layer. As reported in the previous study,[17] the cell containing 5 wt % SiO_2 additive polymer electrolyte showed an overvoltage increase after 700 cycles, and no change of the overvoltage was observed for the sample containing 10 wt % SiO_2 additive electrolyte even after 1000 cycles. The results in Fig. 5 show a constant overvoltage for the samples containing more than 15 wt % SiO_2 additive polymer electrolyte even after 1500 cycles, indicative of high stability with metallic lithium. However, the cells showed an overvoltage increase on cycling time for sample PUA10 (9.1 wt % SiO_2) after 1300 cycles, and for sample PUA (ceramic-free electrolyte) after 550 cycles. The interfacial stability was associated with the structure and morphology of the ceramic-polymer electrolyte, and a dry solvent-free composition. The improved interfacial stability could also be attributed to the dispersed SiO_2 powders that trapped traces of residual impurities and protected the electrode surface. These complementary scavenging and shielding actions were increasingly effective as the amount of nano-SiO_2 powders increased. The schematic model of the Li/ceramic-polymer electrolyte interface could be described like that reported in previous literatures.[22,23]

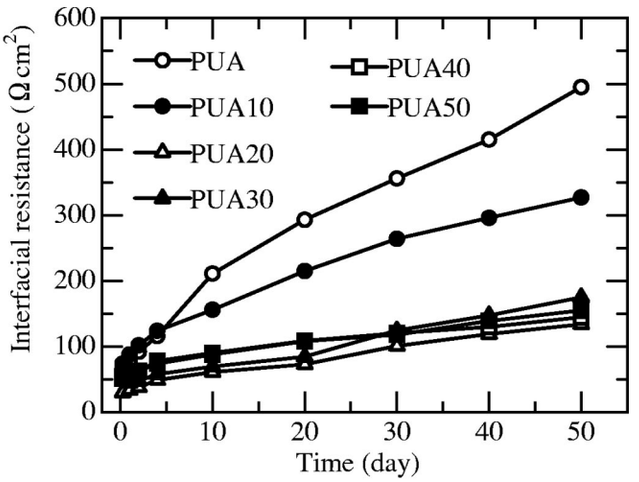

Figure 6. The evolution of interfacial resistances in a symmetric $Li_{0.33}MnO_2$/PAU-SiO_2/ $Li_{0.33}MnO_2$ cell stored in OCV conditions at 60°C.

The storage stability of the interface between composite cathode and the ceramic-polymer electrolyte was evaluated using an ac impedance measurement. The composite cathode consisted of $Li_{0.33}MnO_2$, PEG_{20}-LiTFSI, and carbon (65:30:5 weight ratio). The evolution of the interfacial resistance between the ceramic-polymer electrolyte and the composite cathode are shown in Fig. 6, where the resistances were measured for the cells, composite cathode/PUA-SiO_2/composite cathode, kept under open circuit conditions at 60°C. The results in Fig. 6 show that the interfacial resistance between the electrolyte and the composite cathode increased consistently with time for the sample PUA without any SiO_2 powder; and adding SiO_2 powders to the polymer electrolyte decreased greatly the ascent of the interfacial resistance. There is a reaction between the polymer electrolyte and the composite cathode which was at the charge state (about 3.4 V *vs.* Li^+/Li), resulting in the increase of the interfacial

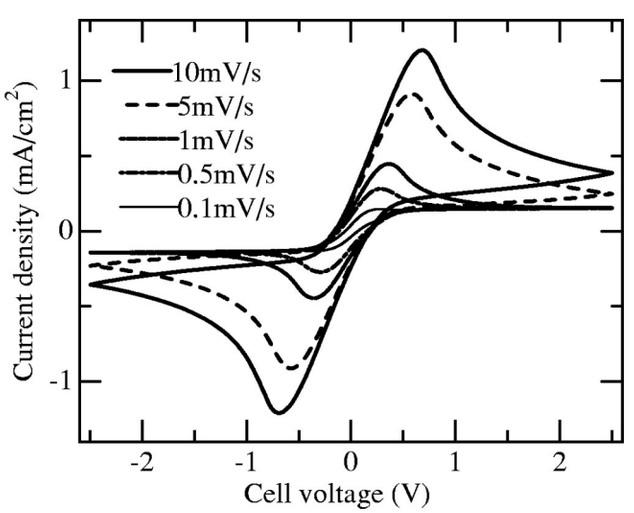

Figure 7. CV of a solid polymer electrolyte (PUA20) sandwiched between two lithium discs at 60°C. Sweep rates were 0.1, 0.5, 1, 5, and 10 mV/s.

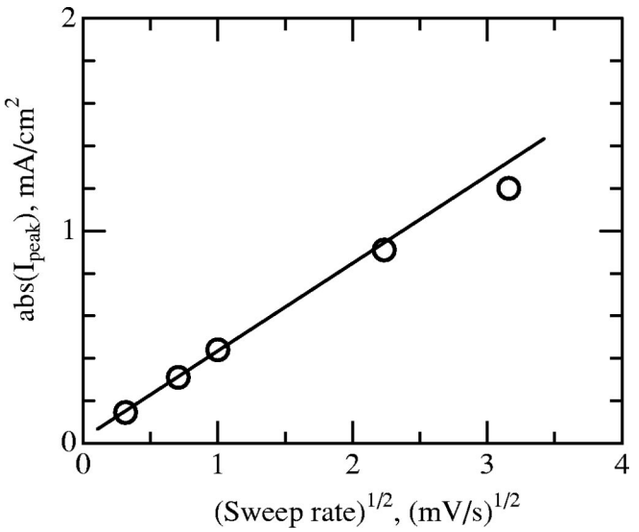

Figure 8. Evaluation of the CV results shown in Fig. 7.

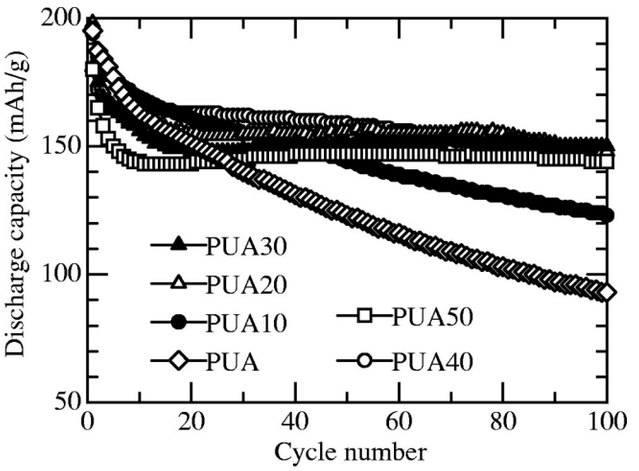

Figure 10. Cyclic performance of ceramic-polymer electrolytes with various amounts of SiO_2 powders at 60°C.

resistance upon time. The addition of SiO_2 powders at a high content would shield and block the reaction, and protect the electrode surface. To our knowledge, there is still no report on improving cathode interface stability from mixing ceramics into polymer electrolytes.

Cyclic voltammetry.—Figure 7 shows cyclic voltammetry (CV) curves of a Li/PUA20/Li cell at a sweep rate from 0.1 mV/s to 10 mV/s. As shown in Fig. 7, the anodic and the cathodic parts of the cycle are symmetric, and the values of the anodic and the cathodic peak currents are almost the same in each cycle. The symmetrical CVs suggest that stripping and plating of lithium be quantitative, and associated with a reversible process. Figure 8 shows the behavior of the I_{peak} *vs.* (sweep rate)$^{1/2}$ plot, where the peak current increases proportionally with the square root of the sweep rate. This is also indirect evidence to the reversible process.

Charge/discharge profile.—Figure 9 shows cycling performance of a Li/$Li_{0.33}MnO_2$ cell using a liquid electrolyte of 1 M $LiN(CF_3SO_2)_2$ in a mixture of ethylene carbonate (EC)/dimethyl carbonate (DMC) (1:2 by volume). The cell was cycled using a constant current of 0.2 mA/cm^2 between 2.0 and 3.5 V at 25°C. The cell has an initial discharge capacity of 180 mAh/g of $Li_{0.33}MnO_2$, corresponding to 0.57 mol Li^+ intercalation into the $Li_{0.33}MnO_2$ framework: $Li_{0.33}MnO_2 + 0.57Li^+ + 0.57e = Li_{0.9}MnO_2$. The result of the cycle life shows that the cell has good rechargeability (even at a slight capacity decay) with a reversible capacity of 140 mAh/g of $Li_{0.33}MnO_2$ for over 100 cycles.

Figure 10 shows the cyclic performance of the Li/ $Li_{0.33}MnO_2$ cells containing solid nano-ceramic polymer electrolytes at a current of 0.05 mA/cm^2 and 60°C. The cells have an initial discharge capacity of 200 mAh/g of $Li_{0.33}MnO_2$, corresponding to 0.67 mol Li^+ intercalation into the $Li_{0.33}MnO_2$ framework: $Li_{0.33}MnO_2 + 0.67Li^+ + 0.67e = LiMnO_2$.

As reported in the previous study,[19] for the sample PUA, the capacity fading during cycling can mainly be ascribed to the fast increase of the interfacial resistance between the polymer electrolyte and the composite cathode, and irreversible structural changes of the cathode material. As shown in Fig. 10, the discharge capacity of sample PUA fades upon cycling with a capacity loss of about 0.5% per cycle. However, the capacity loss decreases with the increase of the ceramic filler content in the polymer electrolyte. A capacity loss of about 0.3% per cycle is observed for sample PUA10. The samples of PUA20, PUA30, PUA40 and PUA50 show excellent charge/discharge properties with a reversible capacity of 150 mAh/g for

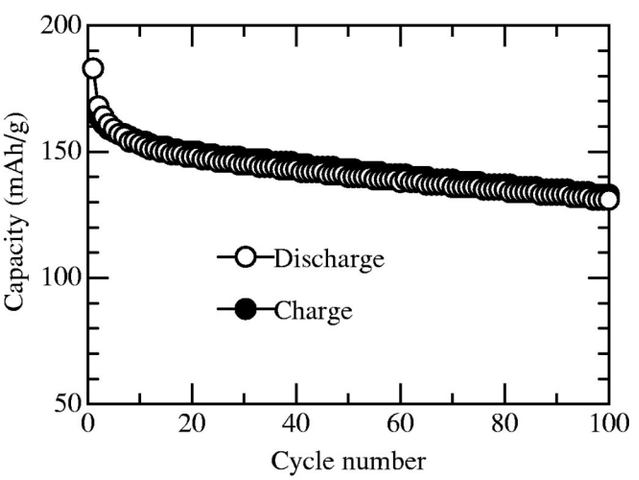

Figure 9. Cyclic performance of a Li/1 M LiTFSI EC-DMC/$Li_{0.33}MnO_2$ cell between 2.0 and 3.5 V at a current of 0.2 mA/cm^2 and at 25°C.

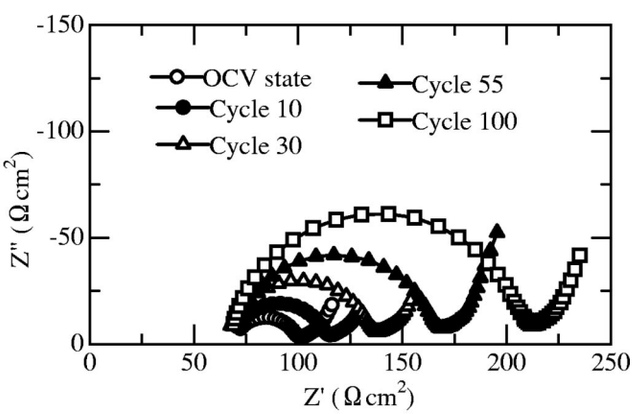

Figure 11. Typical impedance spectra of the Li/PAU30/$Li_{0.33}MnO_2$ cell at various cycles and 60°C.

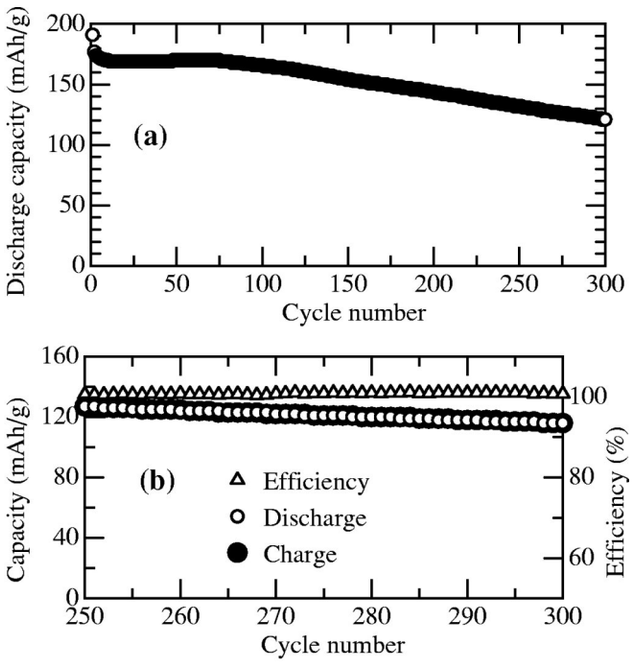

Figure 12. (a) Cycle life, (b) charge-discharge capacity and coulombic efficiency of the Li/PAU30/$Li_{0.33}MnO_2$ cell at 60°C.

over 100 cycles. The good cyclic performance should be attributed to the improved interface between the composite cathode and the ceramic polymer electrolyte (see Fig. 6).

Comparing the cycle life of the cells with the ceramic polymer electrolytes and the liquid electrolyte (see Fig. 9 and 10) shows that the cathode ($Li_{0.33}MnO_2$) cycles better in the liquid electrolyte than in the ceramic-free polymer electrolyte, but best in the nano-ceramic polymer electrolytes containing the high ceramic filler content. This is due to the fact that the Li/electrolyte and cathode/electrolyte interfacial stabilizations provided by the ceramic filler assure a high reversibility of the lithium deposition-stripping process. This can also be explained by the change of the cell resistance upon cycling. The interfacial resistance between the ceramic-free polymer electrolyte and the cathode increases fast with cycling and time. However, the interfacial resistance between the nano-ceramic polymer electrolyte and the cathode increases slowly with cycling and time. These are confirmed by using the ac impedance technique to monitor changes in cell resistance upon charge/discharge cycling. Typical impedance spectra at various cycles are shown in Fig. 11 for sample PUA30. The cell resistance increases about 120 Ωcm^2 after 100 cycles. The value is far less than that in sample PUA. The increase of the cell resistance can be mainly considered as the rise of the impedance of the cathode/electrolyte interface.

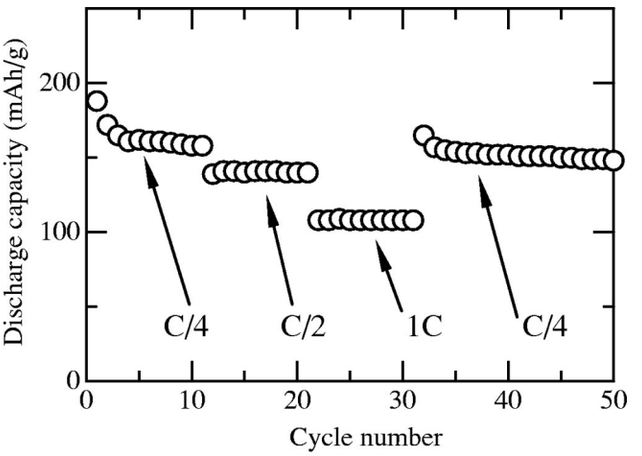

Figure 14. Cyclability of the Li/PAU30/$Li_{0.33}MnO_2$ cell at various charge-discharge rates and 60°C.

Figure 12a shows the cycle life of sample PUA30 with 300 charge-discharge cycles at the very limited capacity decay. Figure 12b demonstrates that these cycles have a coulombic efficiency of about 100% even after long cycles. The cell shows excellent cycling performance and a retention of 70% of the initial capacity after 300 cycles. Such property makes it possible to fabricate an actual all-solid-state lithium polymer battery using the solid-state nano-ceramic polymer electrolyte.

Rate capability.—Figure 13 illustrates discharge curves of a Li/PUA30/$Li_{0.33}MnO_2$ cell at various rates. The cell was charged to 3.5 V at a constant current density of 0.05 mA/cm^2, and was discharged to 2.0 V at various current density from 0.025 to 0.4 mA/cm^2. The

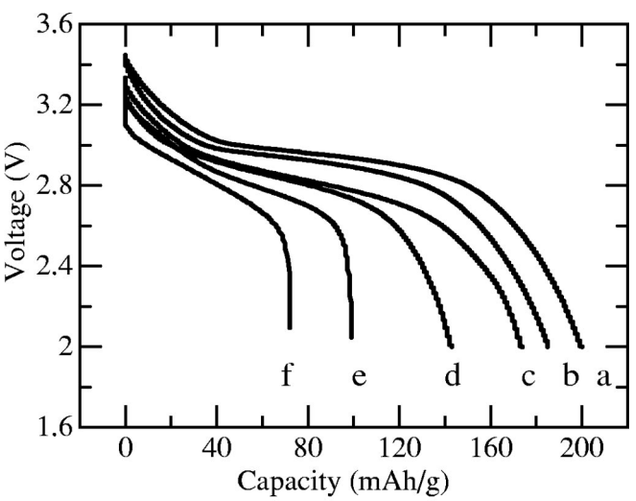

Figure 13. Discharge curves of the Li/PAU30/$Li_{0.33}MnO_2$ cell at various current rates and 60°C. (a) 0.025, (b) 0.05, (c) 0.065, (d) 0.1, (e) 0.2 and (f) 0.4 mA/cm^2.

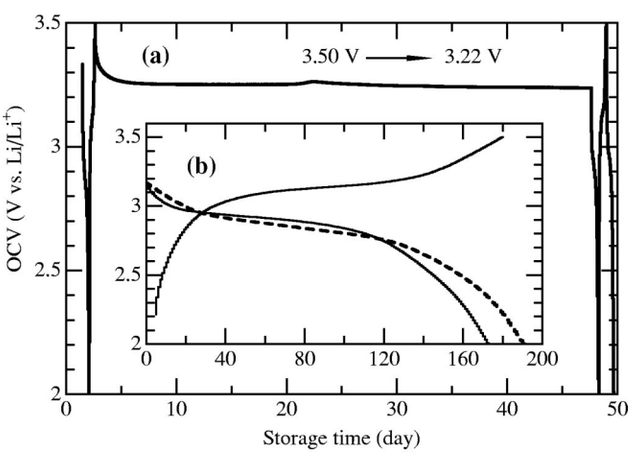

Figure 15. (a) Relationship between OCV of a Li/PAU30/$Li_{0.33}MnO_2$ cell and storage time at 60°C; (b) The first charge-discharge curves (solid lines) and the discharge curve (dotted line) after storage for 45 days.

cell exhibits good rate capacity, and delivers a capacity of about 170 mAh/g at the C/3 rate (0.065 mA/cm^2). Even at a much higher rate, corresponding to the 1C rate (0.2 mA/cm^2), it still delivers a capacity of 100 mAh/g. Figure 14 shows the cyclability of a Li/PUA30/ $Li_{0.33}MnO_2$ cell at various charge-discharge rates. These cycles evolve with a charge-discharge efficiency approaching 100%. This also confirms the smooth and reversible lithium stripping-deposition process as discussed above.

High-temperature storage profile.—The Li/PUA30/ $Li_{0.33}MnO_2$ cell self-discharge at high temperature was also evaluated. The experiment was carried out as follows. The cell was first discharged to 2.0 V at 0.05 mA/cm^2, and charged to 3.5 V. The current was then interrupted, and the voltage was monitored during storage time. After storage for 45 days, the cell was discharged again. Figure 15 shows the change of the OCV as a function of time. The first charge-discharge curves and the discharge curve after storage for 45 days are also given in Fig. 15. The cell voltage drops from 3.50 to 3.25 V during the first 5 days, and then decreased little during further storage. Comparing the first charge capacity with the discharge capacity after storage, the self-discharge loss was 0.05 % per day at 60°C, which is far lower than that in liquid or gel-polymer electrolyte-based lithium-ion batteries.

Conclusions

We report a new type of all-solid-state lithium-polymer battery using a PUA-based nanoceramic-polymer electrolyte in the high ceramic filler content. The composite electrolyte containing more than 20 wt % hydrophilic nano-SiO_2 enhanced its mechanical strength 1000% compared to the ceramic-free electrolyte. The additions of nano-SiO_2 powders in a high concentration protected the electrode surfaces, improved greatly the interfacial stability between Li anode and the electrolyte, or between composite cathode ($Li_{0.33}MnO_2$) and the electrolyte, and gave rise to a further reversible lithium stripping-deposition process. The battery had unique features in terms of cycle life and high-temperature storage. As reported in a previous study,[19] the battery could be operated at a temperature of 40°C, and was thermally stable up to 220°C. These suggest that a practical all-solid-state lithium-polymer battery that can be operated at moderate temperatures (40-60°C) should be attainable.

The National Institute of Advanced Industrial Science and Technology assisted in meeting the publication costs of this article.

References

1. M. Armand, J. M. Chabagno, and M. J. Duclot, in *Fast Ion Transport in Solids*, P. Vashista, J. N. Mundy, and G. K. Shenoy, Editors, p.131, North-Holland, Amsterdam (1979).
2. D. R. Payne and P. V. Wright, *Polymer*, **23**, 690 (1982).
3. F. Croce, G. B. Appetechi, L. Persi, and B. Scrosati, *Nature (London)*, **394**, 456 (1998).
4. J. F. Le Nest, S. Callens, A. Gandini, and M. Armand, *Electrochim. Acta*, **37**, 1585 (1992).
5. M. Watanabe and A. Nishimoto, *Solid State Ionics*, **79**, 306 (1995).
6. P. A. R. D. Jayathilaka, M. A. K. L. Dissanayake, I. Albinsson, and B. E. Mellander, *Electrochim. Acta*, **47**, 3527 (2002).
7. P. P. Prosini, S. Passerini, R. Vellone, and W. H. Smyrl, *J. Power Sources*, **75**, 73 (1998).
8. G. B. Appetecchi, S. Scaccia, and S. Passerini, *J. Electrochem. Soc.*, **147**, 4448 (2000).
9. M. C. Borghini, M. Mastragostino, S. Passerini, and B. Scrosati, *J. Electrochem. Soc.*, **142**, 2118 (1995).
10. H. Y. Sun, H. J. Sohn, O. Yamamoto, Y. Takeda, and N. Imanishi, *J. Electrochem. Soc.*, **146**, 1672 (1999).
11. H. J. Walls, J. Zhou, J. A. Yerian, P. S. Fedkiw, S. A. Khan, M. K. Stowe, and G. L. Baker, *J. Power Sources*, **89**, 156 (2000).
12. E. Quartarone, P. Mustarelli, and A. Magistris, *Solid State Ionics*, **110**, 1 (1998).
13. Y. Matsuo, and J. Kuwano, *Solid State Ionics*, **79**, 295 (1995).
14. C. Capiglia, P. Mustarelli, E. Quartarone, C. Tomasi, and A. Magistris, *Solid State Ionics*, **118**, 73 (1999).
15. Y. Liu, J. Y. Lee, and L. Hong, *J. Power Sources*, **109**, 507 (2002).
16. J. Fan, S. R. Rafhavan, X. Y. Yu, S. A. Khan, P. S. Fedkiw, J. Hou, and G. L. Baker, *Solid State Ionics*, **111**, 117 (1998).
17. G. Jiang, S. Maeda, H. B. Yang, Y. Saito, S. Tanase, and T. Sakai, *J. Power Sources*, In press.
18. Japan Koukai Tokkyo, Jpn. Pat. 2001-35251.
19. G. Jiang, S. Maeda, H. B. Yang, C. Wang, Y. Saito, S. Tanase, and T. Sakai, *J. Electrochem. Soc.*, **151**, A1886 (2004).
20. Y. Xia, K. Tatsumi, T. Fujieda, P. P. Prosini, and T. Sakai, *J. Electrochem. Soc.*, **147**, 2050 (2000).
21. J. Evans, C. A. Vincent, P. G. Bruce, *Polymer*, **28**, 2324 (1987).
22. F. Gray, and M. Armand, in *Energy Storage Systems for Electronics*, T. Osaka and M. Datta, Editors, p. 351, Australia (2000).
23. B. Scrosati, F. Croce, and S. Panero, *J. Power Sources*, **100**, 93 (2001).
24. R. G. Singhal, M. D. Capracotta, J. D. Martin, S. A. Khan, and P. S. Fedkiw, *J. Power Sources*, **128**, 247 (2004).
25. J. Zhou, and P. S. Fedkiw, *Solid State Ionics*, **166**, 275 (2004).